Hindawi
International Journal of Aerospace Engineering
Volume 2020, Article ID 2705175, 9 pages
https://doi.org/10.1155/2020/2705175

Research Article

Flight Stability of Canard-Guided Dual-Spin Projectiles with Angular Rate Loops

Qiushi Zheng and Zhiming Zhou

Beijing Institute of Technology, 10081 Beijing, China

Correspondence should be addressed to Qiushi Zheng; zhengqiushi1993@163.com

Received 25 February 2020; Revised 20 July 2020; Accepted 26 July 2020; Published 7 August 2020

Academic Editor: Paolo Castaldi

Generally, as a precision-guided weapon, the missile has many disadvantage such as high price, difficult maintenance, and low yield. Modern war requires more and more new guided ammunition with high precision, low cost, and low collateral damage. Therefore, as a simple guided conventional ammunition technology, the dual-spin projectile has attracted the attention of ammunition experts recently. This paper proposes a dual-spin projectile scheme based on the rotation control method. Firstly, the concept of the dual-spin projectile is introduced. Secondly, the mathematical model of the dual-spin projectile is established, and the angular motion equation is finally obtained by using some linearized assumptions. Finally, the sufficient and necessary conditions of coning motion stability for dual-spin projectile with angular rate loops are analytically derived and further verified by numerical simulations. It is noticed that the upper bound of the control gain is affected by the delay angle of the control system and the spinning rate of the projectile.

1. Introduction

The trajectory correction projectile is modified from the conventional ammunition, equipped with the ballistic detection device and the correction module. The ballistic detection device measures the trajectory elements and calculates the trajectory deviation in real time during the whole flight. Then, the projectile is guided by canards to reduce the impact miss distance and improve the damage probability. For the two-dimensional rajectory correction, the spin rate of the projectile is a major constraint to the correction effect. Conventional ammunitions always keep a very high spinning rate after launching to maintain the fly gyroscope stability. Thus, it is difficult to use canards to guide the projectile because general actuators do not have such a large operating frequency. In order to solve this problem, a dual-spin configuration principle has been proposed.

The concept of low-cost trajectory correction ammunition first proposed by the United States in the 1970s adopted the dual-spin structure in [1]. The so-called dual-spin structure means that the projectile can be divided into two decoupled parts along the axial direction, which are connected by roller bearings. In the following years, many scholars have studied the dual-spin projectile. Costello and Peterson [2] developed the equations of motion for a dual-spin projectile in atmospheric flight. Guan and Yi [3] established a seven-degree-of-freedom projectile trajectory model for the dual-spin projectile and obtained a more accurate and reliable measurement data by filtering the trajectory of the dual-spin projectile using the UKF algorithm. Burchett et al. [4] obtained the closed form expressions for swerving motion under the action of lateral pulse jets for a dual-spin projectile in atmospheric flight by using the linear theory. Chang et al. [5, 6] studied the spin-rate characteristic of the dual-spin projectile and the dynamic response of the dual-spin projectile under the canard control effect. Liu et al. [7] deduced the analytical expressions without attitude information, which can predict the increment orientation for trajectory angular rate and swerving motion induced by canard control force. Wernert et al. [8] carried out the wind tunnel test of a canards guided 155 mm artillery and got the result of open-loop trajectory simulations.

There has been a considerable literature on the flight stability of conventional spin-stabilized projectiles, such as [9–12]. But for this kind of dual-spin projectiles, there are some differences. Costello and Peterson [2] analysed the stability characteristic of the dual-spin projectile using modified projectile linear theory and obtained the expression of the gyroscopic stability

factor and the dynamic stability factor which take on the same form as the rigid projectile. Wernert [13] addressed the problem of stability of such canard-guided dual-spin-stabilized projectiles and gave the stability criterion considering the influence of canards. He pointed out that the stability for this kind of projectiles is reduced due to the following two factors: the addition of canards and the reduced angular momentum of the forward part. Theodoulis and Wernert [14] present the quasilinear parameter-varying model of the dual-spin-stabilized projectile and analysed the stability of the projectile on different characteristic points of the whole flight envelope. Zhu [15] took account of the control effects of canards and then established a revised stability criterion according to the Hurwitz stability criterion which can be reduced to that of conventional spin-stabilized projectiles.

However, few of the existing literatures have considered the coning motion of dual-spin projectile with the control loop. Thus, this paper focuses on the stability of coning motion for a dual-spin projectile with angular rate loops. The mathematical model of the dual-spin projectile is established. The sufficient and necessary condition of coning motion stability for dual-spin projectile with angular rate loops is analytically derived and further verified by numerical simulations. The stability boundary of control gains is obtained, and moreover, the influence of the total delay angle for the control system and spinning rate of the projectile on stability is analysed.

2. System Configuration

The so-called dual-spin projectile in this paper is improved from a conventional 155 mm spin-stabilized projectile by replacing the original fuse for a novel course correction fuse (CCF), which is illustrated in Figure 1. The projectile can be divided into two parts: the forward part contains the necessary guidance and control hardware and software and the aft part contains the payload. These two parts are connected by rotating bearings and are completely roll decoupled from each other.

As can be seen from Figure 1, the forward part is equipped with two pairs of rotating fins which are used to generate normal force to guide the projectile. After launching, the aft part keeps a high spinning rate of several hundreds of radians per second in order to maintain the fly gyroscopic stability, while the spinning rate of the forward part can be reduced to keep a constant low value in a few seconds under the control of an axial motor. Therefore, this dual-spin structure design can not only solve the technical problems faced by the actuator when the projectile rotates at a high speed but also facilitate the design and normal work of the missile-loading measuring device and can also maintain the gyroscopic stability of the projectile.

3. Mathematical Model

According to the previous studies [2], the 7-DOF equations of motion of the dual-spin projectile are generally established in the body fixed plane (BFP) reference frame, as shown in Figure 2.

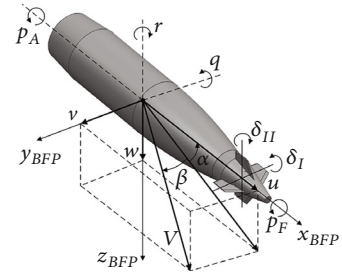

Figure 1: Concept of the dual-spin projectile.

The translational and attitude kinematics in the BFP reference frame can be derived as

$$\begin{bmatrix} \dot{x} \\ \dot{y} \\ \dot{z} \end{bmatrix} = \begin{bmatrix} \cos\theta\cos\psi & -\sin\psi & \sin\theta\cos\psi \\ \cos\theta\sin\psi & \cos\psi & \sin\theta\sin\psi \\ -\sin\theta & 0 & \cos\theta \end{bmatrix} \begin{bmatrix} u \\ v \\ w \end{bmatrix}, \quad (1)$$

$$\begin{bmatrix} \dot{\phi}_f \\ \dot{\phi}_a \\ \dot{\theta} \\ \dot{\psi} \end{bmatrix} = \begin{bmatrix} 1 & 0 & 0 & \tan\theta \\ 0 & 1 & 0 & \tan\theta \\ 0 & 0 & 1 & 0 \\ 0 & 0 & 0 & 1/\cos\theta \end{bmatrix} \begin{bmatrix} p_f \\ p_a \\ q \\ r \end{bmatrix}. \quad (2)$$

The translational and attitude airframe dynamics can be derived in the BFP reference frame as

$$\begin{bmatrix} \dot{u} \\ \dot{v} \\ \dot{w} \end{bmatrix} = \frac{1}{m} \begin{bmatrix} F_x \\ F_y \\ F_z \end{bmatrix} - \begin{bmatrix} 0 & -r & q \\ r & 0 & r\tan\theta \\ -q & -r\tan\theta & 0 \end{bmatrix} \begin{bmatrix} u \\ v \\ w \end{bmatrix}, \quad (3)$$

$$\begin{bmatrix} I_{xf}\dot{p}_f \\ I_{xa}\dot{p}_a \\ I_t\dot{q} \\ I_t\dot{r} \end{bmatrix} = \begin{bmatrix} L_f \\ L_a \\ M \\ N \end{bmatrix} - \begin{bmatrix} 0 \\ 0 \\ \left(I_{xa}p_a + I_{xf}p_f\right)r + I_t r^2\tan\theta \\ -\left(I_{xa}p_a + I_{xf}p_f\right)q - I_t qr\tan\theta \end{bmatrix}, \quad (4)$$

where u, v, and w are the linear velocities, x, y, and z are the linear positions, ϕ_f the roll angle of the forward part, ϕ_a the roll angle of the aft part, θ the pitch angle, ψ the yaw angle, p_f the roll angular rate of the forward part, p_a the roll angular rate of the aft part, and q and r the pitch and yaw angular rate. F_x, F_y, and F_z are the external forces containing aerodynamic and gravity components and can be derived as

$$\begin{bmatrix} F_x \\ F_y \\ F_z \end{bmatrix} = \begin{bmatrix} -QSC_D - mg\sin\theta \\ -QSC_{N\alpha}\beta - QS\left(\frac{L}{V}\right)p_a C_{yp\alpha}\alpha + QSC_{N\delta}\delta_y \\ -QSC_{N\alpha}\alpha + QS\left(\frac{L}{V}\right)p_a C_{yp\alpha}\beta - QSC_{N\delta}\delta_z + mg\cos\theta \end{bmatrix}. \quad (5)$$

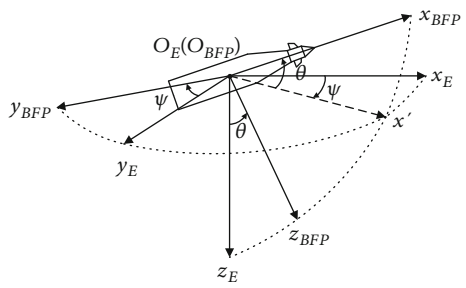

Figure 2: The body fixed plane reference frame.

L_f, L_aM, and N are external moments containing aerodynamic and friction components:

$$\begin{bmatrix} L_f \\ L_a \\ M \\ N \end{bmatrix} = \begin{bmatrix} QSLC_l\delta_l - QSLC_{lpf}\left(\frac{L}{V}\right)p_f + L_{f-a} \\ -QSLC_{lpa}\left(\frac{L}{V}\right)p_a - L_{f-a} \\ QSLC_{m\alpha}\alpha - QSLC_{mq}\left(\frac{L}{V}\right)q - QSL\left(\frac{L}{V}\right)\left(C^f_{np\alpha}p_f + C^a_{np\alpha}p_a\right)\beta + QSLC_{m\delta}\delta_z \\ -QSLC_{m\alpha}\beta - QSLC_{mq}\left(\frac{L}{V}\right)r - QSL\left(\frac{L}{V}\right)\left(C^f_{np\alpha}p_f + C^a_{np\alpha}p_a\right)\alpha + QSLC_{m\delta}\delta_y \end{bmatrix}. \tag{6}$$

The term C_D is the drag coefficient, $C_{N\alpha}$ the lift force coefficient, $C_{l\delta}$ the roll-induced moment coefficient, C_{lpf} the roll-damping moment coefficient of the forward part, C_{lpa} the roll-damping moment coefficient of the aft part, $C_{m\alpha}$ the static moment coefficient, C_{mq} the lateral damping moment coefficient, $C_{np\alpha}$ the Magnus moment coefficient, and $C_{m\delta}$ the canard control moment coefficient. δ_z and δ_y are the equivalent variables of the canard in the pitch and yaw channels.

The definitions of α and β are illustrated in Figure 1 and can be expressed as

$$\begin{aligned} \alpha &= \arctan\left(\frac{w}{u}\right), \\ \beta &= \arctan\left(\frac{v}{V}\right). \end{aligned} \tag{7}$$

Other variables are the mass of the projectile m, the dynamic pressure $Q = 1/2(\rho V^2)$ (where ρ is the air density), the airframe velocity V, the reference area S and length L, the moments of inertia I_{xf}, I_{xa}, and I_t, and the static and viscous friction coefficients C_S and C_V.

It can be seen obviously from Equations (2) and (4) that the longitudinal and lateral dynamics of the dual-spin projectile contain two main couplings. On the one hand, the inertial coupling term $(I_{xa}/I_t)p_a$ greatly depends on the high spin rate of the aft part. On the other hand, the aerodynamic coupling caused by Magnus moments depends on the angle of attack α , angle of sideslip β, and the high spinning rate p_a. Furthermore, the aerodynamic coefficients appearing in Equations (5) and (6) are heavily nonlinear.

4. Angular Motion Equations of the Dual-Spin Projectile

Even though the mathematical model described in Equations (3) and (4) is more accurate and close to the real case, due to the highly nonlinear equations of motion, it is difficult to get the analytical solution and the obvious relationship between the flight characteristics of the missile and control parameters. To facilitate theoretical analysis, the general method is to apply the linearization theory of projectile. This theory has been regarded as an effective tool to analyse the flight stability of projectiles and applied [8–13]. Therefore, in order to linearize these two equations, the following assumptions are introduced firstly:

(1) Relative to the longitudinal velocity u and the angular velocity p_a, variables q, r, v, and w can be regarded as small quantities, so we have $V = \sqrt{u^2 + v^2 + w^2} \approx u$

(2) During a short flight, the varieties of the projectile parameters are neglected, and the velocity and the spinning rates are considered to be constant

(3) The Magnus force and canard control force are negligible quantities compared to aerodynamic forces and the gravity effect is negligible

(4) Angle of attack α and angle of sideslip β are small, so we have $\alpha = \arctan(w/u) \approx w/V$ and $\beta = \arcsin(v/V) \approx v/V$.

Under these assumptions, the lateral equations for the dual-spin projectile can be formulated as

$$\begin{cases} \dot{v} = -\dfrac{QSC_{N\alpha}\beta}{m} - ru \\ \dot{w} = -\dfrac{QSC_{N\alpha}\alpha}{m} + qu \\ \dot{q} = \dfrac{QSL}{I_t}\left[(C_{m\alpha} + C_{m\delta})\alpha + C_{mq}\left(\dfrac{L}{V}\right)q - \left(\dfrac{L}{V}\right)\left(C^f_{np\alpha}p_f + C^a_{np\alpha}p_a\right)\beta + C_{m\delta}\delta_z\right] - \dfrac{\left(I_{xa}p_a + I_{xf}p_f\right)r}{I_t} \\ \dot{r} = \dfrac{QSL}{I_t}\left[-(C_{m\alpha} + C_{m\delta})\beta + C_{mq}\left(\dfrac{L}{V}\right)r - \left(\dfrac{L}{V}\right)\left(C^f_{np\alpha}p_f + C^a_{np\alpha}p_a\right)\alpha + C_{m\delta}\delta_y\right] + \dfrac{\left(I_{xa}p_a + I_{xf}p_f\right)q}{I_t} \end{cases} \tag{8}$$

According to assumptions (1) and (4), we can get

$$\dot{\alpha} \approx \frac{\dot{w} - \alpha \dot{u}}{u} = \frac{QS(-C_{N\alpha} + C_D)}{mV}\alpha + q,$$
$$\dot{\beta} \approx \frac{\dot{v} - \beta \dot{u}}{u} = \frac{QS(-C_{N\alpha} + C_D)}{mV}\beta - r. \tag{9}$$

Thus, we can obtain the lateral equations of the dual-spin projectile in a simplified form as

$$\begin{cases} \dot{\alpha} = -a_1\alpha + q \\ \dot{\beta} = -a_1\beta - r \\ \dot{q} = b_{11}\alpha + b_{12}\beta + b_{21}q - b_{22}r + b_3\delta_z \\ \dot{r} = b_{12}\alpha - b_{11}\beta + b_{22}q + b_{21}r + b_3\delta_y \end{cases}, \tag{10}$$

where

$$a_1 = \frac{QSC_{N\alpha} - QSC_D}{mV},$$
$$b_{11} = \frac{QSL(C_{m\alpha} + C_{m\delta})}{I_t},$$
$$b_{12} = \frac{-QSL^2\left(C_{np\alpha}p_a + C_{np\alpha}p_f\right)/V}{I_t},$$
$$b_{21} = \frac{QSL^2C_{mq}/V}{I_t},$$
$$b_{22} = \frac{I_{xa}p_a + I_{xf}p_f}{I_t},$$
$$b_3 = \frac{QSLC_{m\delta}}{I_t}. \tag{11}$$

By defining the complex variables $\xi = \beta + i\alpha$, $\mu = q + ir$, and $\delta = -\delta_z + i\delta_y$, we can further obtain the angular motion equation of the dual-spin projectile in the complex form as

$$\ddot{\xi} + (a_1 - b_{21} - ib_{22})\dot{\xi} - [b_{11} + a_1b_{21} + i(b_{12} + a_1b_{22})]\xi = ib_3\delta. \tag{12}$$

5. Stability of the Moving Mass Spinning Missile with the Angular Rate Loop

5.1. Dual-Spin Projectile Control System with Angular Rate Loops. The control system with angular rate loops is shown in Figure 3, in which n_y and n_z are control commands, $\dot{\theta}$ and $\dot{\psi}$ are feedback signals which can be measured by IMU mounted on the forward part, k_ω is the control gain, and δ_z and δ_y are equivalent canard deflections.

When the control commands for the pitch and yaw channels are δ_z and δ_y, the ideal equivalent output of the actuator system should also be δ_z and δ_y. However, due to the signal delay, when the actuator system receives the control command, the angular position of the forward part has shifted by $\Delta\gamma_1$. Furthermore, due to the dynamic response delay of the actuator, there will be a certain phase lag in the response output of the actuator system, which causes the actual equivalent output to generate an angular position deviation of $\Delta\gamma_2$. Therefore, the total delay angle of the control system are $\gamma_d = \Delta\gamma_1 + \Delta\gamma_2$.

The actuator system is assumed to be a second-order system, only considering the steady-state output coupling, we can get

$$\begin{bmatrix} \delta_z \\ \delta_y \end{bmatrix} = k_r \begin{bmatrix} \cos\gamma_d & -\sin\gamma_d \\ \sin\gamma_d & \cos\gamma_d \end{bmatrix} \begin{bmatrix} \delta_{cz} \\ \delta_{cy} \end{bmatrix}, \tag{13}$$

$$k_r = \frac{k_s}{\sqrt{\left(1 - T_s^2p_f^2\right)^2 + \left(2\mu_sT_sp_f\right)^2}}, \tag{14}$$

$$\gamma_d = p_f\tau + \arccos\frac{1 - T_s^2p_f^2}{\sqrt{\left(1 - T_s^2p_f^2\right)^2 + \left(2\mu_sT_sp_f\right)^2}}, \tag{15}$$

where T_s is the time constant of the system, μ_s is the damping ratio, k_s is the gain of the servo system, and τ is the command transmission delay time. Obviously, the control action in the pitch channel will cause the movement in the yaw channel, and the control action in the yaw channel will also affect the movement in the pitch channel.

It can be seen from Figure 3 that the input commands to the actuators can be described as

$$\begin{bmatrix} n_{cz} \\ n_{cy} \end{bmatrix} = \begin{bmatrix} -k_\omega & 0 \\ 0 & -k_\omega \end{bmatrix} \begin{bmatrix} -\dot{\theta} \\ \dot{\psi} \end{bmatrix}. \tag{16}$$

According to the definition of coordinate system and angle, positive equivalent canard deflections will generate positive angle of attack and negative angle of sideslip. And the negative angle of attack will generate negative pitching acceleration, and the positive angle of sideslip will generate positive yaw acceleration. Therefore, the displacement instruction of the canard is obtained as

$$\begin{bmatrix} \delta_{cz} \\ \delta_{cy} \end{bmatrix} = \begin{bmatrix} 1 & 0 \\ 0 & 1 \end{bmatrix} \begin{bmatrix} n_{cz} \\ n_{cy} \end{bmatrix}. \tag{17}$$

Meanwhile, based on the assumption that the missile is in horizontal flight, there exists an approximation relationship: $\dot{\alpha} \approx \dot{\theta}$, $\dot{\beta} \approx -\dot{\psi}$. Thus, Equation (17) can be expressed as

$$\begin{bmatrix} \delta_{cz} \\ \delta_{cy} \end{bmatrix} = \begin{bmatrix} -k_\omega & 0 \\ 0 & -k_\omega \end{bmatrix} \begin{bmatrix} \delta_{cz} \\ \delta_{cy} \end{bmatrix}. \tag{18}$$

Finally, substituting Equation (18) into Equation (13), we can get the actual equivalent canard outputs with all the delays as

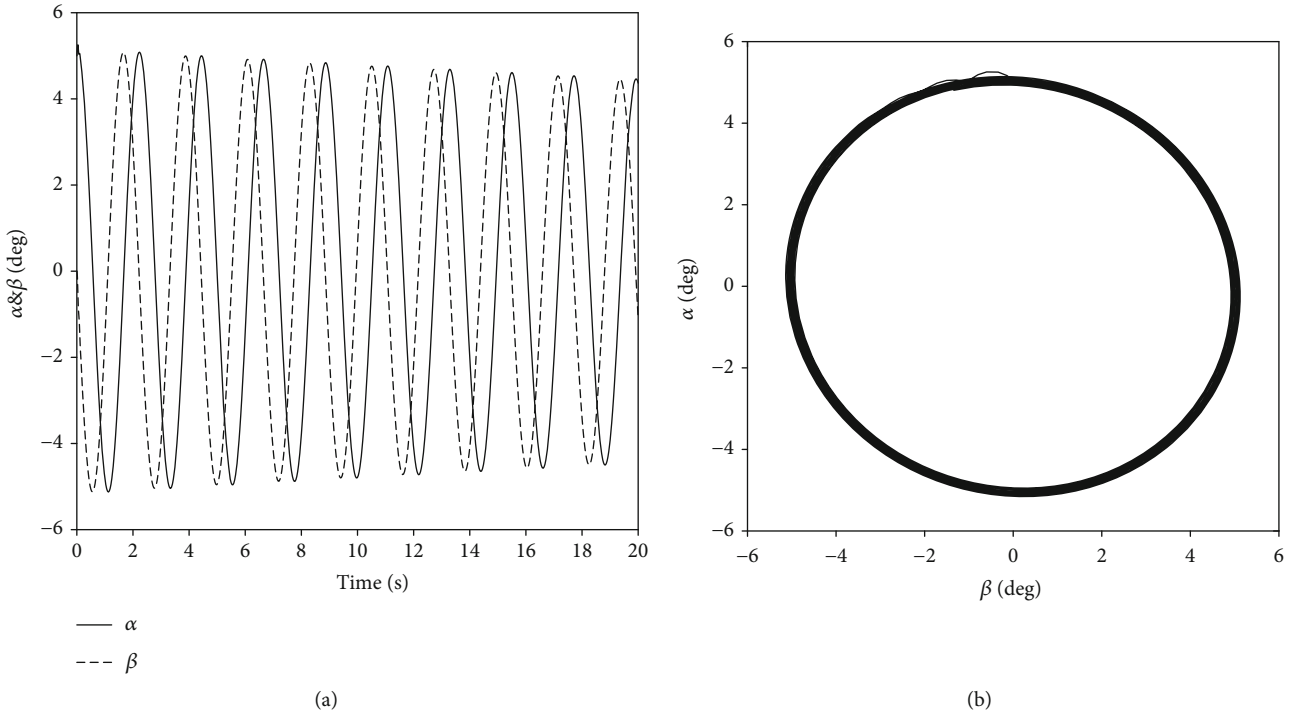

Figure 3: Simulation results for $k_\omega = 0.31$. (a) Curves of angle of attack and sideslip. (b) The critical coning motion.

$$\begin{bmatrix} \delta_z \\ \delta_y \end{bmatrix} = k_r \begin{bmatrix} \cos\gamma_d & -\sin\gamma_d \\ \sin\gamma_d & \cos\gamma_d \end{bmatrix} \begin{bmatrix} \delta_{cz} \\ \delta_{cy} \end{bmatrix}. \tag{19}$$

Converting Equation (19) into the complex form, one has

$$\delta = k_r k_\omega (-\sin\gamma_d + i\cos\gamma_d)\dot{\xi}. \tag{20}$$

5.2. Stability Conditions for the Dual-Spin Projectile Control System. Substituting Equation (20) into the angular motion Equation (12), we can get

$$\ddot{\xi} + [(a_1 - b_{21} + b_3 k_r k_\omega \cos\gamma_d) - i(b_{22} - b_3 k_r k_\omega \sin\gamma_d)]\dot{\xi} - [(b_{11} + a_1 b_{21}) + i(b_{12} + a_1 b_{22})]\xi = 0. \tag{21}$$

Rewrite the above equation into the simplified form as

$$\ddot{\xi} + (H_C - iP_C)\dot{\xi} - (M + iQ) = 0, \tag{22}$$

where

$$H_C = a_1 - b_{21} + b_3 k_r k_\omega \cos\gamma_d, \qquad P_C = b_{22} - b_3 k_r k_\omega \sin\gamma_d. \tag{23}$$

Apparently, the characteristic equation of Equation (22) has the form

$$\lambda^2 + (H_C - iP_C)\lambda - (M + iQ) = 0. \tag{24}$$

Then, we can obtain the characteristic roots as

$$\lambda_{1,2} = \frac{-(H_C - iP_C) \pm \sqrt{(H_C - iP_C)^2 + 4(M + iQ)}}{2}. \tag{25}$$

Assuming that $R_c = R_{cr} + iR_{ci} = (H_C - iP_C)^2 + 4(M + iQ)$, one has

$$R_{cr} = H_C^2 - P_C^2 + 4M, \qquad R_{ci} = -2H_C P_C + 4Q. \tag{26}$$

The real part of $\lambda_{1,2}$ is

$$\lambda_{R(1,2)} = \frac{-H_C \pm \sqrt{(|R| + R_{cr})/2}}{2}, \tag{27}$$

where $|R| = \sqrt{R_{cr}^2 + R_{ci}^2}$; it is obvious that the control system is stable only if the real parts of the characteristic roots are negative, that is

$$-H_C \pm \sqrt{\frac{|R| + R_{cr}}{2}} < 0. \tag{28}$$

The stability condition (28) can be formulated as

$$\begin{cases} -H_C < 0 \\ H_C^2 > \dfrac{|R| + R_{cr}}{2}. \end{cases} \tag{29}$$

By substituting the expressions of these variables, the

necessary and sufficient conditions for the stability of the dual-spin projectile control system can be obtained as

$$\begin{cases} -(L/V)C_{mq} + C_{m\delta}k_r k_\omega \cos\gamma_d > 0 \\ -C_{m\alpha}\left[-(L/V)C_{mq} + C_{m\delta}k_r k_\omega \cos\gamma_d\right]^2 - I_t LC_{np\alpha}^2 p_a^2/QSV^2 + \\ (L/V)C_{np\alpha}p_a\left[-(L/V)C_{mq} + C_{m\delta}k_r k_\omega \cos\gamma_d\right](I_{xa}p_a/QSL - C_{m\delta}k_r k_\omega \sin\gamma_d) > 0. \end{cases} \tag{30}$$

5.3. Stability Analysis. Firstly, by analysing the first inequality in the stability condition (30), which is the pitching damping moment coefficient C_{mq}, it can be seen obviously that when the delay angle $\gamma_d < 90^\circ$, the first inequality is satisfied. When $\gamma_d > 90^\circ$, the control parameter k_ω has a upper limit as follows:

$$k_\omega < \frac{LC_{mq}}{VC_{m\delta}k_r \cos\gamma_d}. \tag{31}$$

Then, analysing the second inequality in the stability condition (30), since the dual-spin projectile is static unstable, we have $C_{m\alpha} > 0$. The first and the second terms of the second inequality are negative; thus, whether the second inequality is true depends on the third term. The magnitude and sign of the third term are mainly affected by the spinning rate of the aft part p_a, the delay angle γ_d, and the control gain k_ω.

The second inequality can be rewritten as a polynomial in terms of k_ω:

$$f(k_\omega) = ak_\omega^2 + bk_\omega + c > 0, \tag{32}$$

where

$$a = k_r^2 C_{m\delta}^2 \cos\gamma_d\left(-C_{m\alpha} - \frac{L}{V}C_{np\alpha}p_a \sin\gamma_d\right),$$

$$b = C_{m\delta}k_r\left[\frac{2L}{V}C_{m\alpha}C_{mq}\cos\gamma d + \left(\frac{L}{V}\right)^2 C_{mq}C_{np\alpha}p_a \sin\gamma_d + \frac{I_{xa}}{QSV}p_a C_{mq}C_{np\alpha}p_a \cos\gamma_d\right], c = -\frac{LC_{np\alpha}p_a^2}{QSV^2}\left(I_t C_{np\alpha} + I_{xa}\right). \tag{33}$$

When $\gamma_d < 90^\circ$, one gets $a < 0$, $b > 0$, and $c < 0$. The two zero points of $f(k_\omega)$ are obtained as

$$0 < k_{\omega 11} = \frac{-b + \sqrt{b^2 - 4ac}}{2a} < k_{\omega 12} = \frac{-b - \sqrt{b^2 - 4ac}}{2a}. \tag{34}$$

Only when $k_{\omega 11} < k_\omega < k_{\omega 12}$ one gets $f(k_\omega) > 0$. The sufficient and necessary condition for the coning motion stability can be derived as

Table 1: Parameters of the 155 mm dual-spin projectile.

Parameter	Value	Parameters	Value
m_s	42.8	I_t	1.893
L	0.155	S	0.01887
V	450	p_a	1450
$C_{m\alpha}$	3.6	C_{mq}	13.2
$C_{m\delta}$	3.6	$C_{np\alpha}$	0.7

$$\frac{-b + \sqrt{b^2 - 4ac}}{2a} < k_\omega < \frac{-b - \sqrt{b^2 - 4ac}}{2a}. \tag{35}$$

When $\gamma_d > 90^\circ$, one gets $a > 0$, $b < 0$, and $c < 0$; the two zero points of $f(k_\omega)$ can be obtained as

$$k_{\omega 21} = \frac{-b - \sqrt{b^2 - 4ac}}{2a} < 0 < k_{\omega 22} = \frac{-b + \sqrt{b^2 - 4ac}}{2a}. \tag{36}$$

Only when $k_\omega < k_{\omega 21}$ or $k_\omega > k_{\omega 22}$ one gets $f(k_\omega) < 0$. The sufficient and necessary condition for the coning motion stability can be derived as

$$\left(k_\omega < \frac{LC_{mq}}{VC_{m\delta}k_r \cos\gamma_d}\right) \cap \left(k_\omega < \frac{-b - \sqrt{b^2 - 4ac}}{2a} \cup k_\omega > \frac{-b + \sqrt{b^2 - 4ac}}{2a}\right). \tag{37}$$

6. Numerical Simulations

To demonstrate the proposed stability condition in the last section, numerical simulations are run for a 155 mm dual-spin projectile. All simulation results are based on a fixed-step (0.001 s), fourth-order Runge–Kutta numerical program by using the MATLAB simulation software. The parameters of the dual-spin projectile are listed in Table 1.

The delay angle of the control system is set as 32.5°; then, the calculated upper bound of the control loop gain can be obtained as 0.31 according to Equation (37). When the control loop gain $k_\omega = 0.23$, which satisfies the stability condition, the simulation results are obtained as shown in Figure 4. It can be seen obviously that the coning motion of the projectile converges to zero quickly. When $k_\omega = 0.31$, which is the critical value, the simulation results are illustrated as shown in

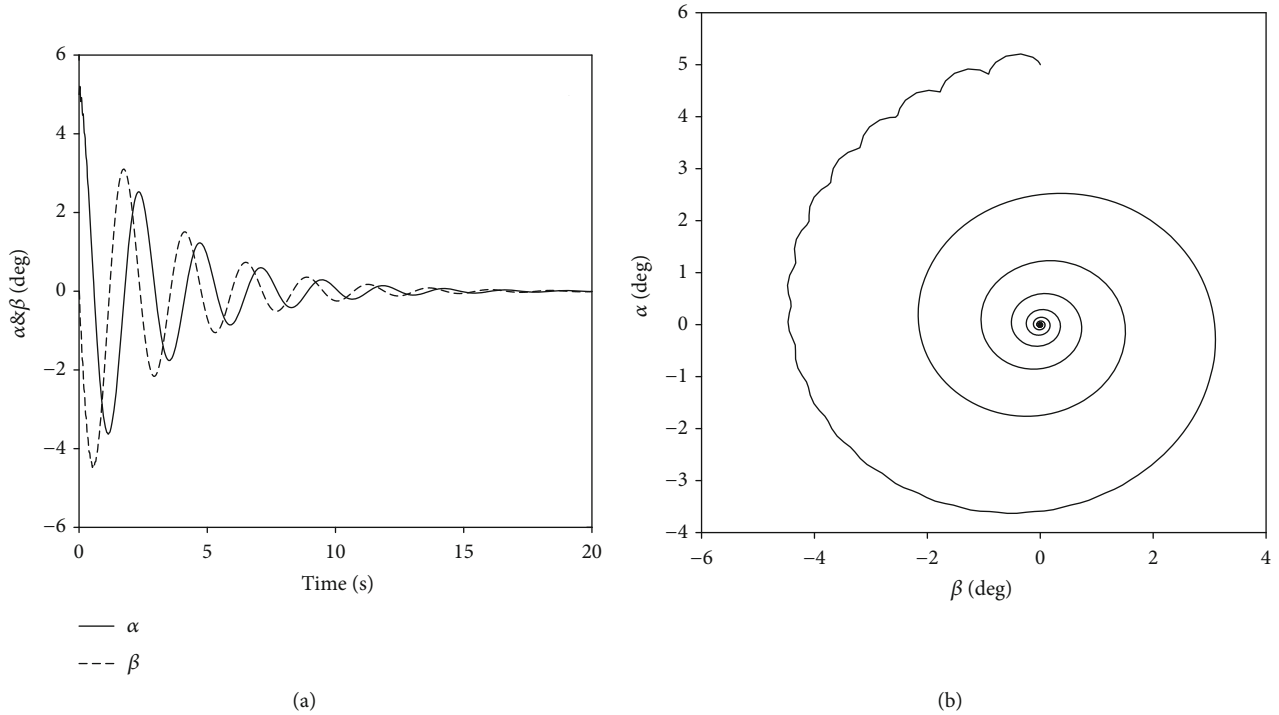

Figure 4: Simulation results for $k_\omega = 0.23$. (a) Curves of angle of attack and sideslip. (b) Stable coning motion.

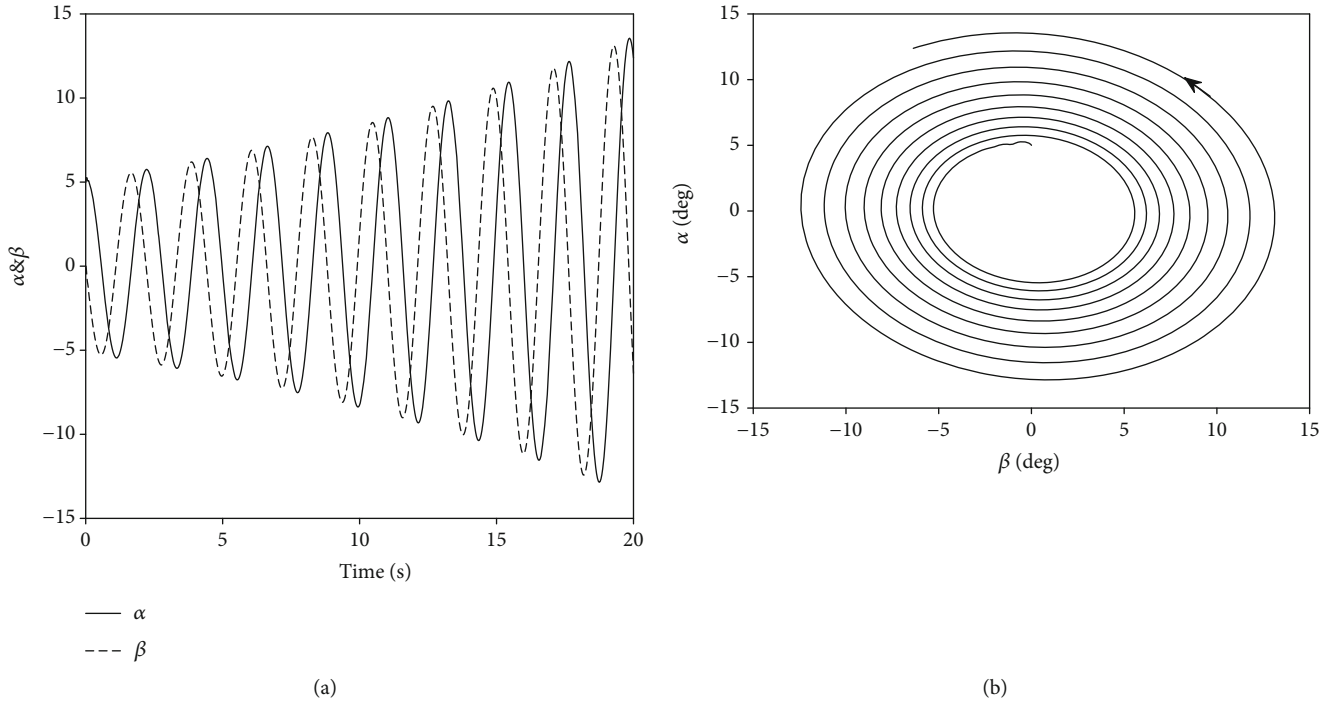

Figure 5: Simulation results for $k_\omega = 0.52$. (a) Curves of angle of attack and sideslip. (b) Unstable coning motion.

Figure 3. It is observed that the coning motion of the missile neither converges nor diverges but presents a critical stable state. When $k_\omega = 0.52$, the simulation results are obtained as shown in Figure 5. It can be seen that the coning motion is divergent.

Furthermore, the influence of the total delay angle of the control system and the spinning rate p_a of the aft part to the stability criterion is demonstrated. The stable regions corresponding to different total delay angles γ_d for the dual-spin projectile control system are illustrated in Figure 6. It can

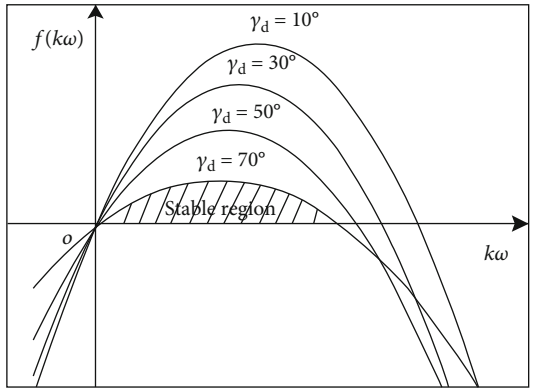

Figure 6: The stable region for different delay angles.

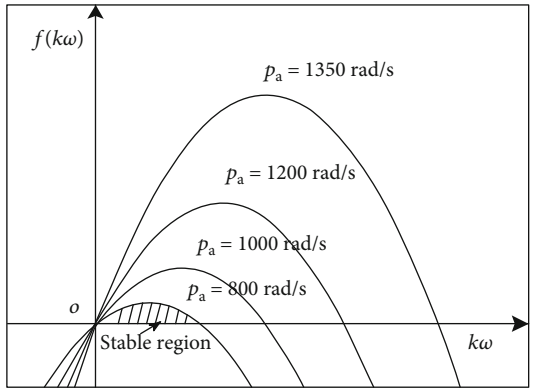

Figure 7: The stable region for different spinning rate of the aft part.

be seen that the stable region of the control system shrinks as the delay angle increases. Therefore, in the design of the control system for the dual-spin projectile, the delay angle should be reduced as far as possible to ensure that the control system is stable.

The stable regions corresponding to different spinning rates p_a of the aft part are illustrated in Figure 7. It is noticed that the stable region of the control system shrinks as the spinning rate decreases. Furthermore, when the spinning rate of the aft part drops to a certain value, any control parameter k_ω cannot guarantee the stability of the dual-spin projectile system. In the actual flight, the spinning rate of the aft part gradually decreases with flight time, which will reduce the stability region of the projectile system. For this reason, the flight stability of the dual-spin projectile is more easily destroyed, which needs to be paid enough attention in the design process.

7. Conclusions

In this paper, the mathematical equation of a dual-spin projectile is established. The sufficient and necessary condition of the coning motion stability for dual-spin projectiles with angular rate loops is analytically derived and further verified by numerical simulations. Simulation results show that there exists a stability boundary value for the control gain. If the control gain exceeds it, the coning motion of the dual-spin projectile will diverge, and the system will become unstable. It is also noticed that as the delay angle increases, the stability region of the system decreases, while, as the spinning rate of the aft part decreases, the stability region of the system decreases greatly. This paper is mainly based on the linearization theory of projectiles, so the stability condition obtained in this paper is applicable to the linearized missile model. In the future, we will focus on the stability analysis of nonlinear model of the dual-spin projectile.

Data Availability

All data, models, and code generated or used during the study appear in the submitted article.

Conflicts of Interest

The authors declare that there is no conflict of interest regarding the publication of this paper.

References

[1] F. J. Reg and J. Smith, "Aeroballistics of a Terminally Corrected Spinning Projectile (TCSP)," *Journal of Spacecraft and Rockets*, vol. 12, no. 12, pp. 733–738, 1975.

[2] M. Costello and A. Peterson, "Linear theory of a dual-spin projectile in atmospheric flight," *Journal of Guidance, Control, and Dynamics*, vol. 23, no. 5, pp. 789–797, 2000.

[3] J. Guan and W. Yi, "Modeling of dual-spinning projectile with canard and trajectory filtering," *International Journal of Aerospace Engineering*, vol. 2018, Article ID 1795158, 7 pages, 2018.

[4] B. Burchett, A. Peterson, and M. Costello, "Prediction of swerving motion of a dual-spin projectile with lateral pulse jets in atmospheric flight," *Mathematical and Computer Modelling*, vol. 35, no. 7-8, pp. 821–834, 2002.

[5] S. Chang, Z. Wang, and T. Liu, "Analysis of spin-rate property for dual-spin-stabilized projectiles with canards," *Journal of Spacecraft and Rockets*, vol. 51, no. 3, pp. 958–966, 2014.

[6] S. Chang, "Dynamic response to canard control and gravity for a dual-spin projectile," *Journal of Spacecraft and Rockets*, vol. 53, no. 3, pp. 558–566, 2016.

[7] X.-d. Liu, D.-g. Li, and Q. Shen, "Swerving orientation of spin-stabilized projectile for fixed-cant canard control input," *Mathematical Problems in Engineering*, vol. 2015, Article ID 173571, 11 pages, 2015.

[8] P. Wernert, F. Leopold, D. Bidino, and J. Juncker, "Wind tunnel tests and open-loop trajectory simulations for a 155 mm canards guided spin stabilized projectile," in *AIAA Atmospheric Flight Mechanics Conference and Exhibit*, Honolulu, Hawaii, August 2008.

[9] C. H. Murphy, *Free Flight Motion of Symmetric Missiles*, Ballistic Research Laboratories, Aberdeen Proving Ground, 1963.

[10] C. H. Murphy, "Angular motion of spinning almost symmetric missiles," *Journal of Guidance, Control and Dynamics*, vol. 2, no. 6, pp. 504–510, 1979.

[11] K. L. Nielsen and J. L. Synge, "On the motion of a spinning shell," *Quarterly of Applied Mathematics*, vol. 4, no. 3, pp. 201–226, 1946.

[12] A. E. Hodapp, "Effect of Mass Asymmetry on Ballistic Match of Projectiles," *Journal of Spacecraft and Rockets*, vol. 13, no. 12, pp. 757–760, 1976.

[13] P. Wernert, "Stability analysis for canard guided dual-spin stabilized projectiles," in *AIAA Atmosphere Flight Mechanics Conference*, Chicago, IIIinois, August 2009.

[14] S. Theodoulis and P. Wernert, "Flight control for a class of 155mm spin-stabilized projectiles with course correction fuse (CCF)," in *AIAA Guidance, Navigation, and Control Conference*, Portland, Oregon, August 2011.

[15] D. Zhu, S. Tang, J. Guo, and R. Chen, "Flight stability of a dual-spin projectile with canards," *Proceedings of the Institution of Mechanical Engineers, Part G: Journal of Aerospace Engineering*, vol. 229, no. 4, pp. 703–716, 2014.